THE NEARLY DEGENERATE TRIPLET ELECTRONIC GROUND STATE ISOMERS OF LITHIUM NITROXIDE

Justin M. TURNEY[1] and Henry F. SCHAEFER III[2,*]

Center for Computational Chemistry, University of Georgia, Athens, Georgia 30602, U.S.A.; e-mail: [1] jturney@ccqc.uga.edu, [2] hfs@uga.edu

Dedicated to the memory of Professor Jaroslav Koutecký.

The triplet electronic ground state potential energy surface of lithium nitroxide has been systematically investigated using convergent quantum mechanical methods. Equilibrium structures and physical properties for five stationary points (three minima and two transition states) have been determined employing highly correlated coupled cluster theory with four correlation-consistent polarized-valence (cc-pVXZ and aug-cc-pVXZ, X = T and Q) and two core correlation-consistent polarized-valence (cc-pCVXZ, X = T and Q) basis sets. The global minimum, roughly L-shaped Li–O–N, is predicted to lie 6.5 kcal mol^{-1} below the linear LiON minimum and 2.4 kcal mol^{-1} below the linear LiON minimum. The barrier to isomerization from the global minimum to LiON was found to be 7.4 kcal mol^{-1} and with regard to LiNO 6.9 kcal mol^{-1}. The dissociation energies, D_0, with respect to Li + NO, have been predicted for all minima and for the global minimum was found to be 34.9 kcal mol^{-1}.
Keywords: Ab initio calculations; Lithium nitroxide; Coupled cluster; Isomerization; Triplet states; IR spectroscopy; Vibrational frequencies.

Lithium nitroxide, a system that has attracted continuing interest over the past five decades, was first prepared in 1957 by Asmussen[1]. The first infrared (IR) study was by Andrews and Pimentel[2] in 1966 using argon matrix isolation techniques. They performed isotopic substitutions at all atomic positions to verify the molecular identity and to conduct a normal-coordinate analysis. Their vibrational frequencies were reported as ν_1 = 1352 cm^{-1}, ν_2 = 333 cm^{-1}, and ν_3 = 650.4 cm^{-1}. From their normal-coordinate analysis they deduced a Li–O–N bond angle of 100 ± 10°, an ON bond length of 1.30 ± 0.05 Å, a LiO bond length of 1.63 Å, and a LiN bond length of 1.66 Å.

Then in 1971, Peslak et al.[3] published the first ab initio study on lithium nitroxide. Using a basis set consisting of six s-type Gaussians on lithium

and 6s + 3p Gaussians on both nitrogen and oxygen they were able to predict a bent structure. The structure they arrived at was in good agreement with respect to bond lengths but their bond angle falls 9° below the lower bound given by Andrews and Pimentel[2] earlier. They assumed that the LiON system is closed-shell singlet but considered the possibility of it being a triplet. Their results suggested that this is the actual case, that Li(NO) is ionic, and it would contain the anion NO⁻ as an approximately identifiable moiety. At that time there was an experimental study by Asmussen[1] that supported their closed shell proposal that reporting Li(NO) as diamagnetic.

In 1973 Tevault and Andrews[4] reexamined the LiON matrix IR spectrum and provided evidence for photoisomerism. The authors report vibrational frequencies of 1352 and 651 cm⁻¹ for a triangular LiON species. They also explain that during mercury photolysis the 651 cm⁻¹ vibration observed disappears and a new 447 cm⁻¹ appears, while the 1352 cm⁻¹ vibrational mode frequency slightly increases, suggesting that the triangular isomer photoisomerized to a bent form.

Girard-Dussau et al.[5] in 1982 used a semi-empirical configuration interaction method with a small basis set to study the LiNO system. In the context of the present paper it should be noted that the results given by Girard-Dussau et. al.[5] for the triplet state do not show a triangular LiON minimum. They conclude that for the triplet system linear LiON is the global minimum, linear LiNO is a local minimum, and there is a transition state with a LiON bond angle of about 30°. They also correctly noted that for the singlet ground state a single determinant method will not accurately describe the system.

A second-order Møller–Plesset (MP2) study was performed by Spoliti et al.[6] on three minima found on the triplet ground state potential energy surface. The reported geometry at their best level of theory (6-311+G* MP2) is r_{LiO} = 2.759 Å, r_{LiN} = 1.9035 Å, r_{ON} = 1.253 Å, and a bond angle of 120.5°.

A more recent study of the LiON system was performed by Vayner and Ball[7] in 2001. Singlet and triplet ground states for LiON were reported with a 6-311+G(d) basis set at the MP2 level of theory. This system has a π^2 valence electron configuration, for which the lowest singlet electronic state ($^1\Delta$) requires (in Cartesian coordinates) a two-determinant reference function. On the other hand, the triplet ground state ($^3\Sigma^-$) can be described by a single determinant, and is expected from Hund's Rules to be the ground state.

From the previous theoretical studies it may be seen that both electron correlation and a sufficient basis set is needed to qualitatively describe this system. In the present study the triplet electronic ground states of the lin-

ear ($\tilde{X}^3\Sigma^-$) and bent ($\tilde{X}^3\text{Å}''$) LiON and the linear ($\tilde{X}^3\Sigma^-$) LiNO isomer of lithium nitroxide have been systematically studied using highly correlated methods available in our laboratory. Special emphasis is placed on the accurate determination of the relative energies for the isomerization between the three minima and dissociation energies for the three isomers into Li (X^2S) atom plus diatomic NO ($X^2\Pi_{1/2}$) with high levels of theory up to single, double, and perturbative triple excitations coupled cluster theory.

THEORETICAL METHODS

Four basis sets were employed in order to optimize structures and determine physical properties of linear and bent LiON and linear LiNO as well as diatomic NO. The basis sets were the correlation-consistent polarized-valence basis sets developed by Dunning and coworkers[8]: cc-pVXZ and aug-cc-pVXZ (X = T, Q). The larger augmented cc-pVXZ sets, designated by aug-cc-pVXZ, include diffuse functions. The latter were only employed for the oxygen and nitrogen atoms.

Core electron correlation on lithium has a much larger effect on predicted molecular properties than does core correlation on N and O. This is most easily understood in terms of the 1s-2s orbital energy differences between Li (2.28 hartrees) and N (14.68 hartrees). To consider the core-correlation effects for lithium in this ionic system the cc-pCVXZ (X = T, Q) type basis sets were used. Given the likelihood that the lithium atom has substantial positive charge in LiNO, an augmented basis set was not used for Li. The largest basis set (aug-cc-pVQZ for N, O and cc-pCVQZ for Li) consists of 215 contracted Gaussian functions for the lithium nitroxide structures. Geometries were optimized with each basis set and level of theory. Harmonic vibrational frequencies were evaluated using analytic methods where available, and otherwise determined through finite differences of analytic gradients or numerical differentiation of total energies.

The electron configuration of the ground state ($X^2\Pi_{1/2}$) of diatomic NO may be described as

$$[\text{core}](3\sigma)^2(4\sigma)^2(5\sigma)^2(1\pi)^4(2\pi) \qquad X^2\Pi_{1/2} \qquad (1)$$

where [core] designates the two core (O–1s-like and N–1s-like) orbitals. For $\tilde{X}^3\Sigma^-$ LiON and LiNO the ground state electron configuration may be described with

$$[\text{core}](4\sigma)^2(5\sigma)^2(6\sigma)^2(1\pi)^4(2\pi)^2 \qquad \tilde{X}^3\Sigma^- \qquad (2)$$

where [core] designates the three core (Li–1s-like, O–1s-like, and N–1s-like) orbitals. Finally, for $\tilde{X}^3A''$ LiON the electron configuration is

$$[core](4a')^2(5a')^2(6a')^2(1a'')^2(7a')^2(8a')(2a'') \qquad \tilde{X}^3A'' \qquad (3)$$

The zeroth-order descriptions for all species were obtained using a single configuration SCF [restricted open-shell Hartree–Fock (ROHF)] wave function. Correlation effects were included using configuration interaction with single and double excitations (CISD), coupled cluster with single and double excitations (CCSD)[9,10], and CCSD with perturbative triples [CCSD(T)][11,12] levels of theory. In the correlated procedures the two core orbitals were frozen for ON and three core orbitals were frozen for LiON. To determine if there is any significant multireference character to this system the complete active space self-consistent field (CASSCF) method was employed. The CASSCF chosen included 14 electrons in 13 orbitals, for a total of 322, 287 for the linear isomers and a total of 644, 490 configuration state functions for the bent isomers, differences are due to symmetry. The smallest of the dominant configuration for any of the isomers made up 92% of the space (both transition states) and the next largest configuration contributing to the system was ~1% (also from the transition states) making it evident that single-reference methods should be able to describe these systems. The MOLPRO[13–15] ab initio program package was utilized during this study.

RESULTS AND DISCUSSION

In Table I total energies and physical properties for the $X^2\Pi_{1/2}$ state of diatomic NO are presented. In Figs 1 and 2 the optimized geometries for $\tilde{X}^3\Sigma^-$ LiON and LiNO are depicted at four levels of sophistication with four basis sets. Total energies and physical properties of these two structures are presented in Tables II and III. Figure 3 provides the optimized geometries for the $\tilde{X}^3A''$ minimum of LiON. Total energies and physical properties for this structure are presented in Table IV. Provided in Figs 4 and 5 are the optimized geometries for the transition states found on this potential energy surface. The total energies and physical properties for these transition states can be found in Table V and VI. Energies relative to the $\tilde{X}^3A''$ global minimum for all other geometries are found in Table VII. Dissociation energies for the minima into Li and NO are located in Table VIII. Total energies for the Li and NO used in the determination of dissociation energies are given in Table IX. A pictorial representation of the potential energy surface of this system is found in Fig. 6.

TABLE I
Total energies (in hartree), dipole moments (in debye), harmonic vibrational frequencies (in cm^{-1}), IR intensities (in parentheses in km mol^{-1}), and ZPVE (in kcal mol^{-1}) for the ground state ($X^2\Pi_{1/2}$) of diatomic NO

Level of theory	Total energy	r_e (NO)	μ_e	ω_e	ZPVE
cc-pVTZ SCF	–129.292 158	1.1141	0.155	2253 (92)	3.22
aug-cc-pVTZ SCF	–129.293 780	1.1139	0.135	2241 (96)	3.20
cc-pVQZ SCF	–129.301 897	1.1125	0.141	2248 (93)	3.21
aug-cc-pVQZ SCF	–129.302 494	1.1125	0.129	2246 (95)	3.21
cc-pVTZ CASSCF	–129.409 406	1.1587			
aug-cc-pVTZ CASSCF	–129.410 768	1.1588			
cc-pVQZ CASSCF	–129.418 862	1.1570			
aug-cc-pVQZ CASSCF	–129.419 361	1.1570			
cc-pVTZ CISD	–129.669 284	1.1373		2076	2.97
aug-cc-pVTZ CISD	–129.676 587	1.1370		2067	2.95
cc-pVQZ CISD	–129.703 066	1.1333		2088	2.98
aug-cc-pVQZ CISD	–129.706 060	1.1330		2085	2.98
cc-pVTZ CCSD	–129.697 891	1.1471		1986	2.84
aug-cc-pVTZ CCSD	–129.706 304	1.1471		1975	2.82
cc-pVQZ CCSD	–129.733 655	1.1432		1996	2.85
aug-cc-pVQZ CCSD	–129.736 995	1.1433		1993	2.85
cc-pVTZ CCSD(T)	–129.717 072	1.1565		1902	2.72
aug-cc-pVTZ CCSD(T)	–129.726 367	1.1569		1889	2.70
cc-pVQZ CCSD(T)	–129.754 601	1.1528		1911	2.73
aug-cc-pVQZ CCSD(T)	–129.758 316	1.1530		1907	2.73
Experiment[a]		1.1508		1904	
Experiment[b]			0.16		

[a] Ref.[16], [b] ref.[21]

|		
cc-pVTZ SCF	1.608	1.261
aug-cc-pVTZ SCF	1.607	1.260
cc-pCVTZ SCF	1.605	1.261
cc-pVQZ SCF	1.603	1.259
aug-cc-pVQZ SCF	1.603	1.258
cc-pCVTZ SCF	1.602	1.259
cc-pVTZ CASSCF	1.630	1.302
aug-cc-pVTZ CASSCF	1.630	1.302
cc-pVQZ CASSCF	1.626	1.300
aug-cc-pVQZ CASSCF	1.627	1.300
cc-pVTZ CISD	1.626	1.265
aug-cc-pVTZ CISD	1.629	1.264
cc-pCVTZ CISD	1.613	1.265
cc-pVQZ CISD	1.621	1.260
aug-cc-pVQZ CISD	1.624	1.259
cc-pCVQZ CISD	1.609	1.259
cc-pVTZ CCSD	1.633	1.273
aug-cc-pVTZ CCSD	1.638	1.273
cc-pCVTZ CCSD	1.620	1.273
cc-pVQZ CCSD	1.629	1.268
aug-cc-pVQZ CCSD	1.632	1.268
cc-pCVQZ CCSD	1.616	1.268
cc-pVTZ CCSD(T)	1.637	1.279
aug-cc-pVTZ CCSD(T)	1.640	1.279
cc-pCVTZ CCSD(T)	1.624	1.279
cc-pVQZ CCSD(T)	1.635	1.274
aug-cc-pVQZ CCSD(T)	1.639	1.274
cc-pCVQZ CCSD(T)	1.620	1.274
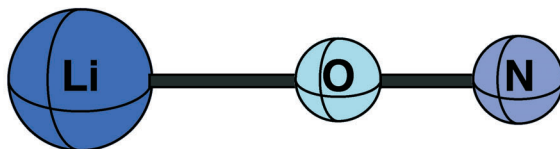
Fig. 1
Predicted geometries for the $\tilde{X}\,^3\Sigma^-$ state of LiON at five levels of theoretical sophistication with six basis sets. Bond lengths are in Å

|		
cc-pVTZ SCF	1.714	1.183
aug-cc-pVTZ SCF	1.715	1.184
cc-pCVTZ SCF	1.712	1.183
cc-pVQZ SCF	1.712	1.182
aug-cc-pVQZ SCF	1.713	1.182
cc-pCVQZ SCF	1.712	1.182
cc-pVTZ CASSCF	1.724	1.235
aug-cc-pVTZ CASSCF	1.728	1.237
cc-pVQZ CASSCF	1.724	1.235
aug-cc-pVQZ CASSCF	1.726	1.235
cc-pVTZ CISD	1.717	1.203
aug-cc-pVTZ CISD	1.721	1.204
cc-pCVTZ CISD	1.706	1.202
cc-pVQZ CISD	1.715	1.200
aug-cc-pVQZ CISD	1.717	1.200
cc-pCVQZ CISD	1.703	1.198
cc-pVTZ CCSD	1.723	1.213
aug-cc-pVTZ CCSD	1.729	1.216
cc-pCVTZ CCSD	1.712	1.213
cc-pVQZ CCSD	1.723	1.211
aug-cc-pVQZ CCSD	1.725	1.212
cc-pCVQZ CCSD	1.709	1.210
cc-pVTZ CCSD(T)	1.726	1.221
aug-cc-pVTZ CCSD(T)	1.733	1.224
cc-pCVTZ CCSD(T)	1.714	1.221
cc-pVQZ CCSD(T)	1.726	1.219
aug-cc-pVQZ CCSD(T)	1.729	1.220
cc-pCVQZ CCSD(T)	1.712	1.218
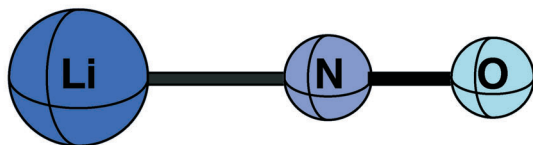
FIG. 2
Predicted geometries for the $\tilde{X}^3\Sigma^-$ state of LiNO at five levels of theoretical sophistication with six basis sets. Bond lengths are in Å

TABLE II

Total energies (in hartree), dipole moments (in debye), harmonic vibrational frequencies (in cm^{-1}), IR intensities (in parentheses in km mol^{-1}), and ZPVE (in kcal mol^{-1}) for the linear equilibrium geometry ($\tilde{X}^3\Sigma^-$ state) of LiON. IR intensities of the ω_2 mode were doubled

Level of theory	Total energy	μ_e	$\omega_1(\sigma^+)$	$\omega_2(\pi)$	$\omega_3(\sigma^+)$	ZPVE
cc-pVTZ SCF	–136.763 310	7.627	1495 (300)	150 (105)	817 (130)	3.73
aug-cc-pVTZ SCF	–136.765 460	7.730	1488 (322)	148 (105)	814 (135)	3.71
cc-pCVTZ SCF	–136.763 703	7.605	1495 (299)	150 (106)	817 (129)	3.73
cc-pVQZ SCF	–136.773 613	7.664	1495 (305)	150 (106)	822 (132)	3.74
aug-cc-pVQZ SCF	–136.774 128	7.714	1494 (320)	147 (104)	820 (135)	3.73
cc-pCVQZ SCF	–136.773 716	7.660	1495 (305)	150 (106)	823 (132)	3.74
cc-pVTZ CASSCF	–136.928 995					
aug-cc-pVTZ CASSCF	–136.931 354					
cc-pVQZ CASSCF	–136.939 992					
aug-cc-pVQZ CASSCF	–136.940 506					
cc-pVTZ CISD	–137.143 504		1472	147	793	3.66
aug-cc-pVTZ CISD	–137.152 709		1465	141	784	3.62
cc-pCVTZ CISD	–137.181 366		1475	151	798	3.68
cc-pVQZ CISD	–137.179 402		1484	146	797	3.68
aug-cc-pVQZ CISD	–137.182 998		1482	141	791	3.65
cc-pCVQZ CISD	–137.219 009		1488	151	807	3.74
cc-pVTZ CCSD	–137.175 325		1430	149	781	3.59
aug-cc-pVTZ CCSD	–137.186 095		1423	142	768	3.54
cc-pCVTZ CCSD	–137.217 993		1430	153	785	3.60
cc-pVQZ CCSD	–137.213 596		1443	147	783	3.60
aug-cc-pVQZ CCSD	–137.217 769		1440	143	776	3.58
cc-pCVQZ CCSD	–137.258 330		1443	153	792	3.63
cc-pVTZ CCSD(T)	–137.192 206		1401	147	772	3.53
aug-cc-pVTZ CCSD(T)	–137.204 431		1391	140	756	3.47
cc-pCVTZ CCSD(T)	–137.235 020		1400	151	777	3.54
cc-pVQZ CCSD(T)	–137.232 775		1411	144	772	3.53
aug-cc-pVQZ CCSD(T)	–137.237 497		1408	140	763	3.50
cc-pCVQZ CCSD(T)	–137.277 686		1412	150	782	3.56

TABLE III
Total energies (in hartree), dipole moments (in debye), harmonic vibrational frequencies (in cm^{-1}), IR intensities (in parentheses in km mol^{-1}), and ZPVE (in kcal mol^{-1}) for the linear equilibrium geometry ($\tilde{X}^3\Sigma^-$ state) of LiNO. IR intensities of the ω_2 mode were doubled

Level of theory	Total energy	μ_e	$\omega_1(\sigma^+)$	$\omega_2(\pi)$	$\omega_3(\sigma^+)$	ZPVE
cc-pVTZ SCF	–136.751 623	7.710	1913 (180)	231 (77)	745 (223)	4.46
aug-cc-pVTZ SCF	–136.754 177	7.877	1896 (191)	225 (80)	741 (235)	4.41
cc-pCVTZ SCF	–136.751 912	7.699	1913 (179)	230 (78)	746 (222)	4.46
cc-pVQZ SCF	–136.761 955	7.777	1906 (188)	228 (81)	747 (230)	4.44
aug-cc-pVQZ SCF	–136.762 747	7.850	1901 (192)	226 (80)	744 (235)	4.43
cc-pCVQZ SCF	–136.762 028	7.774	1906 (188)	228 (81)	745 (229)	4.44
cc-pVTZ CASSCF	–136.919 526					
aug-cc-pVTZ CASSCF	–136.923 301					
cc-pVQZ CASSCF	–136.931 332					
aug-cc-pVQZ CASSCF	–136.932 405					
cc-pVTZ CISD	–137.146 275		1795	222	740	4.26
aug-cc-pVTZ CISD	–137.155 892		1784	213	732	4.21
cc-pCVTZ CISD	–137.183 914		1803	226	746	4.29
cc-pVQZ CISD	–137.182 488		1802	218	741	4.26
aug-cc-pVQZ CISD	–137.186 256		1799	215	737	4.24
cc-pCVQZ CISD	–137.221 908		1811	224	750	4.30
cc-pVTZ CCSD	–137.179 954		1707	212	727	4.09
aug-cc-pVTZ CCSD	–137.190 938		1691	205	716	4.03
cc-pCVTZ CCSD	–137.222 537		1710	217	733	4.11
cc-pVQZ CCSD	–137.218 443		1713	211	727	4.09
aug-cc-pVQZ CCSD	–137.222 655		1707	207	722	4.06
cc-pCVQZ CCSD	–137.263 135		1717	216	735	4.12
cc-pVTZ CCSD(T)	–137.199 110		1650	211	722	4.00
aug-cc-pVTZ CCSD(T)	–137.211 508		1631	203	709	3.93
cc-pCVTZ CCSD(T)	–137.241 859		1653	215	729	4.02
cc-pVQZ CCSD(T)	–137.239 914		1653	209	721	3.99
aug-cc-pVQZ CCSD(T)	–137.244 664		1646	205	715	3.96
cc-pCVQZ CCSD(T)	–137.284 802		1657	215	730	4.02

Geometries

The equilibrium bond length for the ground state ($X^2\Pi_{1/2}$) of diatomic NO is experimentally determined to be r_e(ON) = 1.15077 Å [16] and is in good agreement with the predicted bond length of 1.153 Å. The theoretically predicted NO bond length generally increases with advanced treatments of correlation effects and decreases with larger basis sets. The inclusion of the diffuse function on both atoms shortens the ON bond distance at all levels of theory.

For the local minimum linear LiON isomer, including electron correlation through coupled cluster methods yields a general trend of increasing LiO and ON bond lengths (Fig. 1). These bond lengths are shortened with increasing basis set size. The inclusion of the diffuse functions on N and O increases the bond lengths. A previous theoretical study[7] predicted r_e(LiO) = 1.648 Å and r_e(NO) = 1.274 Å with the 6-311+G(d) MP2 method compared to the present study, in which r_e(LiO) = 1.639 Å and r_e(NO) = 1.274 Å, aug-cc-pVQZ CCSD(T).

The linear LiNO isomer follows a similar trend as that for linear LiON. Advanced treatments of electron correlation yield an elongation of both LiN and NO bond distances (Fig. 2). The bond lengths contract with increasing basis set, but inclusion of diffuse functions lengthens the bonds. For linear LiNO Vayner and Ball[7] predicted r_e(LiN) = 1.724 Å and r_e(ON) = 1.223 Å with 6-311+G(d) MP2 compared to the present results, r_e(LiN) = 1.729 Å and r_e(ON) = 1.220 Å with aug-cc-pVQZ CCSD(T). The NO bond length in LiNO is increased as well, though not as much as in LiON.

The bent global minimum $\tilde{X}^3A''$ LiON structures are shown in Fig. 3. With inclusion of electron correlation the LiO and ON bond lengths increase, while the LiON angle decreases by ~6°. The $\tilde{X}^3A''$ LiO bond distance is longer (by 1.813 – 1.639 = 0.174 Å) than that for linear LiON. As for the $\tilde{X}^3A''$ ON equilibrium separation, compared to linear Li–ON, this bond distance is reasonably consistent. However, for linear Li–NO the NO distance is significantly longer (1.275 – 1.220 = 0.055 Å) than for the $\tilde{X}^3A''$ state. When compared to the previous theoretical work[7] [r_e(LiO) = 1.841 Å, r_e(ON) = 1.271 Å, and α_e(LiON) = 72° with 6-311+G(d) MP2] the present results are qualitatively consistent [r_e(LiO) = 1.813 Å, r_e(ON) = 1.275 Å, and α_e(LiON) = 73.6° with aug-cc-pVQZ CCSD(T)]. The agreement between the present theoretical predictions (73.5°) and the experimental bond angle (100 ± 10°) is poor. Given the large number of independent theoretical methods used here, the experimental result should be re-examined.

| cc-pVTZ SCF | 1.741 | | 1.248 |
aug-cc-pVTZ SCF	1.741		1.248
cc-pCVTZ SCF	1.738		1.248
cc-pVQZ SCF	1.736		1.247
aug-cc-pVQZ SCF	1.737		1.246
cc-pCVQZ SCF	1.735		1.247
cc-pVTZ CASSCF	1.794		1.295
aug-cc-pVTZ CASSCF	1.796	79.6	1.295
cc-pVQZ CASSCF	1.789	79.6	1.293
aug-cc-pVQZ CASSCF	1.790	79.7	1.293
		79.7	
cc-pVTZ CISD	1.791	79.7	1.257
aug-cc-pVTZ CISD	1.795	79.7	1.256
cc-pCVTZ CISD	1.778		1.256
cc-pVQZ CISD	1.785	75.0	1.252
aug-cc-pVQZ CISD	1.788	75.0	1.251
cc-pCVQZ CISD	1.771	75.1	1.250
		75.1	
cc-pVTZ CCSD	1.802		1.271
aug-cc-pVTZ CCSD	1.808	74.8	1.271
cc-pCVTZ CCSD	1.789	74.9	1.272
cc-pVQZ CCSD	1.798	74.8	1.266
aug-cc-pVQZ CCSD	1.801	74.9	1.266
cc-pCVQZ CCSD	1.782	75.0	1.266
		74.9	
cc-pVTZ CCSD(T)	1.813		1.280
aug-cc-pVTZ CCSD(T)	1.820	74.1	1.280
cc-pCVTZ CCSD(T)	1.799	74.2	1.280
cc-pVQZ CCSD(T)	1.809	74.0	1.275
aug-cc-pVQZ CCSD(T)	1.813	74.3	1.275
cc-pCVQZ CCSD(T)	1.793	74.4	1.275
		74.1	
		73.4	
		73.5	
		73.3	
		73.5	
		73.6	
		73.4	
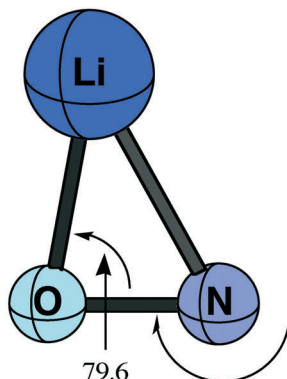
Fɪɢ. 3
Predicted geometries for the $\tilde{X}\,^3A''$ state of LiON at five levels of theoretical sophistication with six basis sets. Bond lengths are in Å and angles in degrees

TABLE IV
Total energies (in hartree), dipole moments (in debye), harmonic vibrational frequencies (in cm^{-1}), IR intensities (in parentheses in km mol^{-1}), and ZPVE (in kcal mol^{-1}) for the bent equilibrium geometry ($\tilde{X}^3A''$ state) of LiON

Level of theory	Total energy	μ_e	$\omega_1(a')$	$\omega_2(a')$	$\omega_3(a')$	ZPVE
cc-pVTZ SCF	–136.761 790	6.368	1490 (214)	323 (34)	743 (151)	3.65
aug-cc-pVTZ SCF	–136.764 080	6.429	1484 (222)	320 (35)	738 (154)	3.63
cc-pCVTZ SCF	–136.762 113	6.354	1489 (214)	322 (34)	742 (149)	3.65
cc-pVQZ SCF	–136.772 113	6.376	1490 (217)	323 (35)	747 (149)	3.66
aug-cc-pVQZ SCF	–136.772 715	6.411	1489 (222)	321 (36)	744 (153)	3.65
cc-pCVQZ SCF	–136.772 213	6.375	1490 (217)	323 (35)	747 (150)	3.66
cc-pVTZ CASSCF	–136.935 560					
aug-cc-pVTZ CASSCF	–136.937 977					
cc-pVQZ CASSCF	–136.946 536					
aug-cc-pVQZ CASSCF	–136.947 118					
cc-pVTZ CISD	–137.150 428		1493	372	705	3.67
aug-cc-pVTZ CISD	–137.159 462		1488	367	696	3.65
cc-pCVTZ CISD	–137.188 166		1498	377	710	3.70
cc-pVQZ CISD	–137.186 224		1507	372	707	3.70
aug-cc-pVQZ CISD	–137.189 754		1505	368	703	3.68
cc-pCVQZ CISD	–137.225 771		1512	378	716	3.72
cc-pVTZ CCSD	–137.184 533		1408	373	695	3.54
aug-cc-pVTZ CCSD	–137.194 772		1402	365	683	3.50
cc-pCVTZ CCSD	–137.227 272		1407	380	700	3.55
cc-pVQZ CCSD	–137.222 489		1422	373	696	3.56
aug-cc-pVQZ CCSD	–137.226 432		1420	368	690	3.66
cc-pCVQZ CCSD	–137.267 340		1421	381	705	3.58
cc-pVTZ CCSD(T)	–137.203 196		1366	373	688	3.47
aug-cc-pVTZ CCSD(T)	–137.214 633		1358	364	674	3.53
cc-pCVTZ CCSD(T)	–137.246 136		1365	381	694	3.49
cc-pVQZ CCSD(T)	–137.243 342		1377	373	688	3.49
aug-cc-pVQZ CCSD(T)	–137.247 724		1375	367	681	3.46
cc-pCVQZ CCSD(T)	–137.288 408		1377	381	697	3.51
Experimental[a]			1352	333	650.4	
Experimental[b]			1352		651	
Experimental[c]			1351		651	
Experimental[d]			1351.0		651.7	

[a] Ref.[2], [b] ref.[4], [c] ref.[18], [d] ref.[22]

Figure 4 shows the transition state structure for isomerization between $\tilde{X}^3A''$ LiON and $\tilde{X}^3\Sigma^-$ LiON (denoted as LiON TS). Figure 5 reports the transition state structure between $\tilde{X}^3A''$ LiON and $\tilde{X}^3\Sigma^-$ LiNO (denoted as LiNO TS) at four levels of theoretical sophistication with four basis sets. The LiON TS has a bond angle of 130°, which is closer to the linear LiON structure. This feature is consistent with the Hammond postulate[17], which states that the transition state should have a structure closer to that of the reactant for an exothermic process. In regard to the LiNO TS the Hammond postulate does not hold, because the LiNO transition state is closer to triangular LiON.
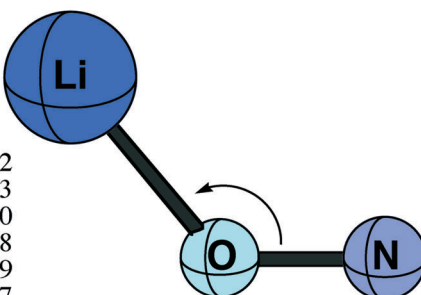
The inclusion of the 1s core electrons on lithium results in a shortening of the Li–X (X = O, N) bond lengths for all conformations at the correlated levels. This effect can be surprisingly large, as may be seen for the $\tilde{X}^3A''$ state by comparing the Li–N distance [cc-pVQZ CCSD(T) value 1.809 Å] without core correlation to the value 1.793 predicted with the cc-pCVQZ CCSD(T) method. The bond angles found in the bent minimum and transition states do not show significant changes with the use of the core-correlated basis sets.

Harmonic Vibrational Frequencies

The harmonic vibrational frequency for the $X^2\Pi_{1/2}$ ground state of diatomic NO has been experimentally determined[16] to be 1904 cm^{-1}. The harmonic vibrational frequency from the present coupled cluster methods is in good agreement with the experimental values; specifically, we predict ω_e = 1907 for the aug-cc-pVQZ CCSD(T) method.

The three harmonic vibrational frequencies for the $\tilde{X}^3\Sigma^-$ LiON system are also predicted to be lowered with the correlated wave functions relative to those with the SCF method, reflecting the longer LiO and ON bond lengths with correlated methods. The three correlated methods employed [CISD, CCSD, and CCSD(T)] present very similar vibrational frequencies. The predicted frequencies for the linear Li–ON structure at the aug-cc-pVQZ CCSD(T) level of theory (Table II) are ω_1 = 1408 cm^{-1}, ω_2 = 140 cm^{-1}, and ω_3 = 763 cm^{-1}.

For the $\tilde{X}^3\Sigma^-$ Li–NO structure the three harmonic vibrational frequencies are predicted to decrease with the correlated wave functions relative to the SCF results as well. This decrease reflects the longer LiN and NO bond distances with the correlated methods. The predicted frequencies for the linear Li–NO structure at the aug-cc-pVQZ CCSD(T) level of theory are ω_1 = 1646 cm^{-1}, ω_2 = 205 cm^{-1}, and ω_3 = 715 cm^{-1}.

cc-pVTZ SCF	1.682	111.1
aug-cc-pVTZ SCF	1.683	111.2
cc-pCVTZ SCF	1.680	111.0
cc-pVQZ SCF	1.678	111.1
aug-cc-pVQZ SCF	1.679	111.1
cc-pCVQZ SCF	1.677	111.1
	1.268	
cc-pVTZ CASSCF	1.693	1.267	123.4
aug-cc-pVTZ CASSCF	1.694	1.268	123.9
cc-pVQZ CASSCF	1.689	1.266	123.5
aug-cc-pVQZ CASSCF	1.690	1.265	123.8
	1.266	
cc-pVTZ CISD	1.682		124.2
aug-cc-pVTZ CISD	1.687	1.311	124.2
cc-pCVTZ CISD	1.672	1.311	123.5
cc-pVQZ CISD	1.679	1.309	124.1
aug-cc-pVQZ CISD	1.681	1.308	124.3
cc-pCVQZ CISD	1.667		123.5
	1.276	
cc-pVTZ CCSD	1.682	1.274	128.7
aug-cc-pVTZ CCSD	1.689	1.275	128.4
cc-pCVTZ CCSD	1.671	1.270	128.1
cc-pVQZ CCSD	1.680	1.269	128.3
aug-cc-pVQZ CCSD	1.683	1.269	128.4
cc-pCVQZ CCSD	1.667		127.7
	1.286	
cc-pVTZ CCSD(T)	1.683	1.284	130.6
aug-cc-pVTZ CCSD(T)	1.692	1.286	130.1
cc-pCVTZ CCSD(T)	1.671	1.280	130.0
cc-pVQZ CCSD(T)	1.682	1.279	130.1
aug-cc-pVQZ CCSD(T)	1.686	1.280	130.2
cc-pCVQZ CCSD(T)	1.668		129.5
	1.292	
	1.291	
	1.292	
	1.286	
	1.286	
	1.292	

Fɪɢ. 4

Predicted geometries for the $\tilde{X}\,^3A''$ transition state of LiON at five levels of theoretical sophistication with six basis sets. Bond lengths are in Å and angles in degrees

cc-pVTZ SCF	114.2	1.792
aug-cc-pVTZ SCF	113.7	1.795
cc-pCVTZ SCF	114.0	1.791
cc-pVQZ SCF	113.6	1.792
aug-cc-pVQZ SCF	113.5	1.793
cc-pCVQZ SCF	113.6	1.791
cc-pVTZ CASSCF	125.0	1.798
aug-cc-pVTZ CASSCF	122.9	1.805
cc-pVQZ CASSCF	123.0	1.801
aug-cc-pVQZ CASSCF	122.5	1.804
cc-pVTZ CISD	112.3	1.793
aug-cc-pVTZ CISD	111.3	1.799
cc-pCVTZ CISD	112.0	1.783
cc-pVQZ CISD	111.3	1.793
aug-cc-pVQZ CISD	111.0	1.796
cc-pCVQZ CISD	111.2	1.781
cc-pVTZ CCSD	113.1	1.797
aug-cc-pVTZ CCSD	113.1	1.797
cc-pCVTZ CCSD	112.9	1.787
cc-pVQZ CCSD	111.9	1.798
aug-cc-pVQZ CCSD	111.6	1.802
cc-pCVQZ CCSD	111.8	1.785
cc-pVTZ CCSD(T)	113.4	1.799
aug-cc-pVTZ CCSD(T)	111.9	1.809
cc-pCVTZ CCSD(T)	113.2	1.788
cc-pVQZ CCSD(T)	112.1	1.801
aug-cc-pVQZ CCSD(T)	111.7	1.806
cc-pCVQZ CCSD(T)	112.0	1.787

O—N bond lengths (Å):

1.207
1.208
1.207
1.206
1.206
1.206

1.258
1.260
1.258
1.259

1.229
1.229
1.228
1.225
1.225
1.224

1.242
1.242
1.242
1.239
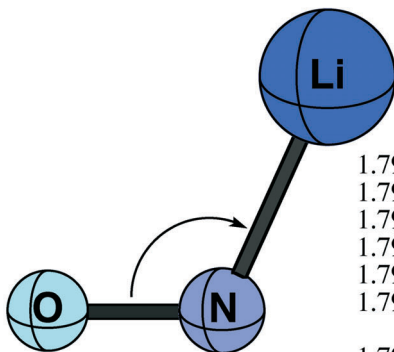1.239
1.238

1.251
1.253
1.251
1.248
1.249
1.248

Fig. 5
Predicted geometries for the $\tilde{X}\,^3A''$ transition state of LiNO at five levels of theoretical sophistication with six basis sets. Bond lengths are in Å and angles in degrees

TABLE V
Total energies (in hartree), dipole moments (in debye), harmonic vibrational frequencies (in cm^{-1}), IR intensities (in parentheses in km mol^{-1}), and ZPVE (in kcal mol^{-1}) for the isomerization transition state ($\tilde{X}^3A''$) of LiON

Level of theory	Total energy	μ_e	$\omega_1(a')$	$\omega_2(a')$	$\omega_3(a')$	ZPVE
cc-pVTZ SCF	–136.758 555	7.438	1423 (220)	182i	808 (153)	3.19
aug-cc-pVTZ SCF	–136.760 929	7.511	1419 (235)	179i	802 (156)	3.17
cc-pCVTZ SCF	–136.758 932	7.415	1423 (219)	183i	807 (152)	3.19
cc-pVQZ SCF	–136.768 924	7.450	1425 (224)	182i	811 (153)	3.20
aug-cc-pVQZ SCF	–136.769 603	7.487	1425 (235)	180i	808 (156)	3.19
cc-pCVQZ SCF	–136.769 036	7.446	1425 (224)	182i	811 (153)	3.20
cc-pVTZ CASSCF	–136.927 013					
aug-cc-pVTZ CASSCF	–136.929 602					
cc-pVQZ CASSCF	–136.938 131					
aug-cc-pVQZ CASSCF	–136.938 813					
cc-pVTZ CISD	–137.140 498		1418	178i	780	3.14
aug-cc-pVTZ CISD	–137.149 964		1413	173i	768	3.12
cc-pCVTZ CISD	–137.178 156		1431	174i	776	3.16
cc-pVQZ CISD	–137.176 447		1432	178i	781	3.16
aug-cc-pVQZ CISD	–137.180 224		1431	174i	776	3.16
cc-pCVQZ CISD	–137.215 853		1436	183i	791	3.18
cc-pVTZ CCSD	–137.172 720		1377	178i	769	3.07
aug-cc-pVTZ CCSD	–137.183 728		1370	170i	754	3.04
cc-pCVTZ CCSD	–137.215 208		1375	182i	773	3.07
cc-pVQZ CCSD	–137.211 040		1390	176i	769	3.09
aug-cc-pVQZ CCSD	–137.215 373		1388	172i	762	3.07
cc-pCVQZ CCSD	–137.255 576		1389	181i	778	3.10
cc-pVTZ CCSD(T)	–137.189 817		1348	178i	762	3.02
aug-cc-pVTZ CCSD(T)	–137.202 256		1339	169i	744	2.98
cc-pCVTZ CCSD(T)	–137.232 471		1346	182i	767	3.02
cc-pVQZ CCSD(T)	–137.230 430		1359	176i	760	3.03
aug-cc-pVQZ CCSD(T)	–137.234 293		1356	171i	752	3.01
cc-pCVQZ CCSD(T)	–137.275 144		1357	182i	770	3.04

The harmonic vibrational frequencies for the $\tilde{X}\,^3A''$ LiON global minimum at the aug-cc-pVQZ CCSD(T) level of theory (Table IV) are $\omega_1 = 1375$ cm^{-1}, $\omega_2 = 367$ cm^{-1}, and $\omega_3 = 681$ cm^{-1}. These may be compared with the 1966 Andrews–Pimentel experimental[2] values $\nu_1 = 1352$ cm^{-1}, $\nu_2 = 333$ cm^{-1}, and $\nu_3 = 650$ cm^{-1}, or the more recent Andrews et al.[18] experimental values of $\nu_1 = 1351$ cm^{-1} and $\nu_3 = 651$ cm^{-1}. Considering that the experimental frequencies are fundamentals and the theoretical results harmonic, the agreement is quite good, especially when one realizes the anharmonicity will decrease the harmonic frequencies. The $\tilde{X}\,^3A''$ NO stretching frequency (1351 cm^{-1}) shows a significant reduction relative to that of diatomic NO (1907 cm^{-1}) and is slightly smaller than that predicted for linear LiON (1408 cm^{-1}). This feature is consistent with Badger's rule[19,20], that the larger force constant (high vibrational frequency) may be associated with the shorter bond length.

Harmonic vibrational frequencies for the LiON transition state are provided in Table V. The predicted frequencies at the aug-cc-pVQZ CCSD(T) level of theory are $\omega_1 = 1356$ cm^{-1}, $\omega_2 = 171i$ cm^{-1}, and $\omega_3 = 752$ cm^{-1}. The LiO stretching frequency ω_1 for the transition state is lower than that for the linear LiON molecule, reflecting the longer bond distance.

The LiNO transition state harmonic vibrational frequencies are presented in Table VI. The predicted frequencies at the aug-cc-pVQZ CCSD(T) level of theory are $\omega_1 = 1497$ cm^{-1}, $\omega_2 = 230i$ cm^{-1}, and $\omega_3 = 701$ cm^{-1}. The lower LiN stretching frequency ω_3 for this transition state lies below that for the linear LiNO molecule, reflecting the longer LiN bond length.

Energetics

Relative energies between the ground states of the three lithium nitroxide isomers are given in Table VII. With the aug-cc-pVQZ basis set the classical relative energies T_e for the linear LiON with respect to the bent global minimum LiON are predicted to be [at the aug-cc-pVQZ CCSD(T) level of theory] 6.4 kcal mol^{-1}; for the LiON transition state 7.8 kcal mol^{-1}; for linear LiNO 1.9 kcal mol^{-1}; for the LiNO transition state 7.2 kcal mol^{-1}. The energy separation generally increases for Li–ON and the LiON transition state but decreases for Li–NO and for the LiNO transition state with advanced treatments of electron correlation. The inclusion of zero-point vibrational energy (ZPVE) lowers the relative energy for the linear minima and raises it for the transition states. Compared to a previous theoretical study[7] our relative energies are higher for the secondary minima [previous work: linear LiON 6.2 kcal mol^{-1} and linear LiNO 0.8 kcal mol^{-1}, 6-311+G(d) MP2]. With

TABLE VI
Total energies (in hartree), dipole moments (in debye), harmonic vibrational frequencies (in cm^{-1}), IR intensities (in parentheses in km mol^{-1}), and ZPVE (in kcal mol^{-1}) for the isomerization transition state ($\tilde{X}\,^3A''$) of LiNO

Level of theory	Total energy	μ_e	$\omega_1(a')$	$\omega_2(a')$	$\omega_3(a')$	ZPVE
cc-pVTZ SCF	–136.742 444	7.887	1753 (156)	257i	722 (152)	3.54
aug-cc-pVTZ SCF	–136.745 264	8.000	1738 (170)	253i	716 (155)	3.51
cc-pCVTZ SCF	–136.742 729	7.870	1753 (155)	256i	722 (151)	3.54
cc-pVQZ SCF	–136.752 829	7.918	1746 (164)	256i	722 (151)	3.53
aug-cc-pVQZ SCF	–136.753 714	7.976	1742 (169)	254i	718 (154)	3.52
cc-pCVQZ SCF	–136.752 899	7.918	1746 (164)	256i	722 (151)	3.53
cc-pVTZ CASSCF	–136.917 143					
aug-cc-pVTZ CASSCF	–136.920 779					
cc-pVQZ CASSCF	–136.928 755					
aug-cc-pVQZ CASSCF	–136.929 813					
cc-pVTZ CISD	–137.136 963		1658	245i	725	3.41
aug-cc-pVTZ CISD	–137.146 835		1647	241i	714	3.38
cc-pCVTZ CISD	–137.174 271		1666	250i	729	3.42
cc-pVQZ CISD	–137.173 096		1667	244i	724	3.42
aug-cc-pVQZ CISD	–137.177 028		1663	244i	719	3.40
cc-pCVQZ CISD	–137.212 135		1674	249i	732	3.44
cc-pVTZ CCSD	–137.171 294		1566	237i	714	3.25
aug-cc-pVTZ CCSD	–137.182 532		1548	234i	713	3.23
cc-pCVTZ CCSD	–137.213 568		1556	241i	719	3.25
cc-pVQZ CCSD	–137.209 696		1563	237i	713	3.25
aug-cc-pVQZ CCSD	–137.214 087		1557	234i	707	3.24
cc-pCVQZ CCSD	–137.254 019		1563	242i	721	3.27
cc-pVTZ CCSD(T)	–137.190 548		1500	234i	710	3.16
aug-cc-pVTZ CCSD(T)	–137.203 183		1482	228i	696	3.11
cc-pCVTZ CCSD(T)	–137.232 982		1500	238i	716	3.17
cc-pVQZ CCSD(T)	–137.231 264		1503	233i	708	3.16
aug-cc-pVQZ CCSD(T)	–137.236 182		1497	230i	701	3.14
cc-pCVQZ CCSD(T)	–137.275 771		1504	239i	717	3.17

Relative energies of the (LiNO) structures with respect to the triangular global minimum (in kcal mol^{-1}) with ZPVE corrected values in parentheses

Level of theory	Relative energy				
	$\widetilde{X}\,^3\Sigma^-$ LiON	$\widetilde{X}\,^3$A″ TS1	$\widetilde{X}\,^3$A″ LiON	$\widetilde{X}\,^3$A″ TS2	$\widetilde{X}\,^3\Sigma^-$ LiNO
cc-pVTZ SCF	–0.95 (–0.87)	2.03 (1.57)	0.00	12.14 (12.03)	6.38 (7.19)
aug-cc-pVTZ SCF	–0.87 (–0.79)	1.98 (1.52)	0.00	11.81 (11.69)	6.21 (6.99)
cc-pCVTZ SCF	–1.00 (–0.92)	2.00 (1.53)	0.00	12.16 (12.05)	6.40 (7.21)
cc-pVQZ SCF	–0.94 (–0.86)	2.00 (1.54)	0.00	12.10 (11.97)	6.37 (7.15)
aug-cc-pVQZ SCF	–0.89 (–0.81)	1.95 (1.49)	0.00	11.92 (11.79)	6.26 (7.04)
cc-pCVQZ SCF	–0.94 (–0.86)	1.99 (1.53)	0.00	12.12 (11.99)	6.39 (7.17)
cc-pVTZ CISD	4.34 (4.33)	6.23 (5.70)	0.00	8.45 (8.19)	2.61 (3.20)
aug-cc-pVTZ CISD	4.24 (4.21)	5.96 (5.43)	0.00	7.92 (7.65)	2.24 (2.80)
cc-pCVTZ CISD	4.27 (4.25)	6.28 (5.74)	0.00	8.72 (8.45)	2.67 (3.26)
cc-pVQZ CISD	4.28 (4.26)	6.14 (5.60)	0.00	8.24 (7.96)	2.34 (2.90)
aug-cc-pVQZ CISD	4.24 (4.21)	5.98 (5.46)	0.00	7.99 (7.71)	2.20 (2.76)
cc-pCVQZ CISD	4.24 (4.23)	6.22 (5.68)	0.00	8.56 (8.27)	2.42 (3.00)
cc-pVTZ CCSD	5.78 (5.83)	7.41 (6.94)	0.00	8.31 (8.02)	2.87 (3.42)
aug-cc-pVTZ CCSD	5.44 (5.48)	6.93 (6.47)	0.00	7.68 (7.41)	2.41 (2.94)
cc-pCVTZ CCSD	5.82 (5.88)	7.57 (7.09)	0.00	8.60 (8.30)	2.97 (3.53)
cc-pVQZ CCSD	5.58 (5.62)	7.18 (6.71)	0.00	8.03 (7.72)	2.54 (3.07)
aug-cc-pVQZ CCSD	5.44 (5.36)	6.94 (6.35)	0.00	7.75 (7.33)	2.37 (2.77)
cc-pCVQZ CCSD	5.65 (5.71)	7.38 (6.90)	0.00	8.36 (8.05)	2.64 (3.18)
cc-pVTZ CCSD(T)	6.90 (6.96)	8.40 (7.95)	0.00	7.94 (7.63)	2.56 (3.09)
aug-cc-pVTZ CCSD(T)	6.40 (6.34)	7.77 (7.22)	0.00	7.18 (6.76)	1.96 (2.36)
cc-pCVTZ CCSD(T)	6.98 (7.03)	8.58 (8.11)	0.00	8.25 (7.93)	2.68 (3.21)
cc-pVQZ CCSD(T)	6.63 (6.67)	8.10 (7.64)	0.00	7.58 (7.25)	2.15 (2.65)
aug-cc-pVQZ CCSD(T)	6.42 (6.45)	7.80 (7.35)	0.00	7.24 (6.92)	1.92 (2.42)
cc-pCVQZ CCSD(T)	6.73 (6.78)	8.32 (7.85)	0.00	7.93 (7.60)	2.26 (2.77)

the consideration of the core-correlated basis sets, the changes in relative energies are all less than 0.35 kcal mol^{-1}. The largest relative energy change occurs for the Li–NO transition state. This stationary point (TS2) lies 7.58 kcal above the $\tilde{X}^3A''$ global minimum with cc-pVQZ CCSD(T), but at 7.93 kcal with cc-pCVQZ CCSD(T).

The ZPVE corrected potential surface for the isomerization reaction

linear LiON ← LiON TS ← triangular LiON → LiNO TS → linear LiNO

is presented in Fig. 6 at the cc-pVQZ CCSD(T) level of sophistication. This surface was constructed by varying the Li–O–N bond angle by five-degree increments and allowing the bonds to relax. The activation energy for the reaction triangular LiON → LiON TS is predicted to be 7.35 kcal mol^{-1} and for triangular LiON → LiNO TS 6.92 kcal mol^{-1}. For the reverse reaction, back to triangular LiON, the activation energy is 0.90 kcal mol^{-1} for linear LiON and 4.50 kcal mol^{-1} for linear LiNO.

Dissociation energies for the formation of Li and ON are provided in Table VIII. For the roughly L-shaped isomer the energy to dissociation is 34.9 kcal mol^{-1}, for linear LiON it is 28.4 kcal mol^{-1}, and for linear LiNO it is 32.4 kcal mol^{-1}. The inclusion of electron correlation increases the dissociation energy by about 10 kcal mol^{-1} for each isomer. With larger ba-
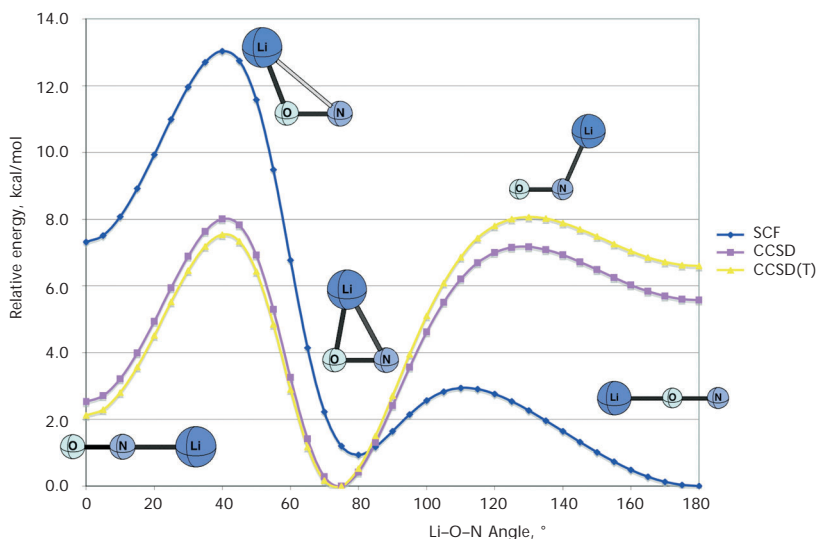

FIG. 6
Diagrammatic potential energy surfaces of LiON obtained with the cc-pVQZ basis set

TABLE VIII
Dissociation energies of linear and bent LiON and linear LiNO into atomic Li (^{2}S) plus NO ($X\,^2\Pi_{1/2}$) (in kcal mol^{-1}) with ZPVE corrected values in parentheses

Level of theory	D_e (D_0) triangular Li–ON	D_e (D_0) linear Li–ON	D_e (D_0) linear Li–NO
cc-pVTZ SCF	23.19 (22.76)	24.14 (23.63)	16.81 (15.57)
aug-cc-pVTZ SCF	23.61 (23.18)	24.47 (23.97)	17.39 (16.19)
cc-pCVTZ SCF	23.39 (22.96)	24.39 (23.88)	16.99 (15.75)
cc-pVQZ SCF	23.54 (23.10)	24.49 (23.96)	17.17 (15.94)
aug-cc-pVQZ SCF	23.55 (23.11)	24.43 (23.92)	17.29 (16.07)
cc-pCVQZ SCF	23.61 (23.16)	24.55 (24.02)	17.22 (15.99)
cc-pVTZ CISD	30.41 (29.71)	26.07 (25.38)	27.81 (26.51)
aug-cc-pVTZ CISD	31.50 (30.80)	27.26 (26.60)	29.26 (28.00)
cc-pCVTZ CISD	28.02 (27.30)	23.76 (23.04)	25.36 (24.03)
cc-pVQZ CISD	31.67 (30.95)	27.39 (26.69)	29.32 (28.05)
aug-cc-pVQZ CISD	32.00 (31.30)	27.76 (27.09)	29.81 (28.55)
cc-pCVQZ CISD	29.10 (28.36)	24.86 (24.13)	26.68 (25.36)
cc-pVTZ CCSD	33.86 (33.16)	28.08 (27.33)	30.99 (29.74)
aug-cc-pVTZ CCSD	35.01 (34.33)	29.56 (28.85)	32.60 (31.40)
cc-pCVTZ CCSD	34.61 (33.90)	28.79 (28.02)	31.64 (30.37)
cc-pVQZ CCSD	35.23 (34.52)	29.65 (28.90)	32.69 (31.45)
aug-cc-pVQZ CCSD	35.61 (34.79)	30.17 (29.44)	33.24 (32.02)
cc-pCVQZ CCSD	35.99 (35.26)	30.34 (29.56)	33.35 (32.08)
cc-pVTZ CCSD(T)	33.54 (32.79)	26.64 (25.83)	30.97 (29.69)
aug-cc-pVTZ CCSD(T)	34.88 (34.05)	28.48 (27.71)	32.92 (31.69)
cc-pCVTZ CCSD(T)	34.40 (33.63)	27.42 (26.60)	31.71 (30.41)
cc-pVQZ CCSD(T)	35.17 (34.41)	28.54 (27.74)	33.02 (31.76)
aug-cc-pVQZ CCSD(T)	35.59 (34.85)	29.17 (28.40)	33.67 (32.43)
cc-pCVQZ CCSD(T)	36.04 (35.27)	29.32 (28.49)	33.78 (32.49)

sis sets the dissociation energies also increase. Inclusion of lithium 1s core-correlation does not meaningfully alter the dissociation energy, as seen in Table VIII. Dissociation into Li$^+$ and NO$^-$ is a significantly higher energy process than into neutral Li and NO, and this ionic pathway is not expected to be competitive in the gas phase, because the ionization potential of Li is much greater than the electron affinity of NO.

Table IX
Total energies (in hartree) for Li (^{2}S) and NO ($X^2\Pi_{1/2}$)

Level of theory	Li (^{2}S)	NO ($X^2\Pi_{1/2}$)
cc-pVTZ SCF	–7.432 679	–129.292 158
aug-cc-pVTZ SCF		–129.293 780
cc-pCVTZ SCF	–7.432 679	
cc-pVQZ SCF	–7.432 695	–129.301 897
aug-cc-pVQZ SCF		–129.302 494
cc-pCVQZ SCF	–7.432 695	
cc-pVTZ CISD		–129.669 284
aug-cc-pVTZ CISD		–129.676 587
cc-pCVTZ CISD	–7.474 224	
cc-pVQZ CISD		–129.703 066
aug-cc-pVQZ CISD		–129.706 060
cc-pCVQZ CISD	–7.476 330	
cc-pVTZ CCSD		–129.697 891
aug-cc-pVTZ CCSD		–129.706 304
cc-pCVTZ CCSD	–7.474 226	
cc-pVQZ CCSD		–129.733 655
aug-cc-pVQZ CCSD		–129.736 995
cc-pCVQZ CCSD	–7.476 333	
cc-pVTZ CCSD(T)		–129.717 072
aug-cc-pVTZ CCSD(T)		–129.726 367
cc-pCVTZ CCSD(T)	–7.474 248	
cc-pVQZ CCSD(T)		–129.754 601
aug-cc-pVQZ CCSD(T)		–129.758 316
cc-pCVQZ CCSD(T)	–7.476 367	

CONCLUSIONS

The triplet electronic ground state isomers ($\tilde{X}^3\Sigma^-$ and $\tilde{X}^3A''$ LiON, and $\tilde{X}^3\Sigma^-$ LiNO) of lithium nitroxide have been studied using convergent quantum mechanical methods. It was demonstrated that the global minimum is the approximately L-shaped Li-O-N structure at coupled cluster levels of theory. At the aug-cc-pVQZ CCSD(T) level the $\tilde{X}^3A''$ state of LiON is predicted to have the following harmonic vibrational frequencies $\omega_1 = 1375$ cm^{-1}, $\omega_2 = 367$ cm^{-1}, and $\omega_3 = 681$ cm^{-1}, which compare well to the Andrews and Pimentel's experimental fundamental frequencies[2] $\nu_1 = 1352$ cm^{-1}, $\nu_2 = 333$ cm^{-1}, and $\nu_3 = 650$ cm^{-1}, respectively. Triangular (roughly L-shaped) LiON is predicted to lie 6.5 kcal mol^{-1} below linear LiON and 2.4 kcal mol^{-1} below linear LiNO. The dissociation energy to Li + NO is predicted to be 34.9 kcal mol^{-1} for triangular LiON, 28.4 kcal mol^{-1} for linear LiON, and 32.4 kcal mol^{-1} for linear LiNO. Although LiON is an ionic system, consideration of the core effects of lithium does not significantly change the predictions reported here.

REFERENCES

1. Asmussen R. W.: *Acta Chem. Scand.* **1957**, *11*, 1435.
2. Andrews L., Pimentel G. C.: *J. Chem. Phys.* **1966**, *44*, 2361.
3. Peslak J., Klett D. S., David C. W.: *J. Am. Chem. Soc.* **1970**, *93*, 5001.
4. Tevault D. E., Andrews L.: *J. Chem. Phys.* **1973**, *77*, 1640.
5. Girard-Dussau N., Dargelos A., Chaillet M.: *J. Mol. Struct.* **1982**, *89*, 123.
6. Spoliti M., Ramondo F., Diomedi-Camassei F., Bencivenni L.: *J. Mol. Struct.* **1994**, *312*, 41.
7. Vayner E., Ball D. W.: *J. Mol. Struct.* **2001**, *542*, 149.
8. Dunning T. H.: *J. Chem. Phys.* **1989**, *90*, 1007.
9. Purvis G. D., Bartlett R. J.: *J. Chem. Phys.* **1982**, *98*, 1358.
10. Rittby M., Bartlett R. J.: *J. Phys. Chem.* **1988**, *92*, 3033.
11. Raghavachari K., Trucks G. W., Pople J. A., Head-Gordon M.: *Chem. Phys. Lett.* **1989**, *157*, 479.
12. Scuseria G. E.: *Chem. Phys. Lett.* **1991**, *176*, 27.
13. Amos R. D., Bernhardsson A., Berning A., Celani P., Cooper D. L., Deegan M. J. O., Dobbyn A. J., Eckert F., Hampel C., Hetzer G., Knowles P. J., Korona T., Lindh R., Lloyd A. W., McNicholas S. J., Manby F. R., Meyer W., Mura M. E., Nickass A., Palmieri P., Pitzer R. M., Rauhut G., Schütz U., Schumann U., Stoll H., Stone A. J., Tarroni R., Thorsteinsson T., Werner H.-J.: *MOLPRO*, a package of ab initio programs designed by H.-J. Werner and P. J. Knowles, version 2002.1.

14. Werner H.-J., Knowles P. J.: *J. Chem. Phys.* **1985**, *82*, 5053.
15. Knowles P. J., Werner H.-J.: *Chem. Phys. Lett.* **1985**, *115*, 259.
16. Huber K. P., Herzberg G.: *Constants of Diatomic Molecules*. Van Nostrand Reinhold, New York 1979.
17. Hammond G. S.: *J. Am. Chem. Soc.* **1955**, *77*, 334.
18. Andrews L., Zhou M., Wang X.: *J. Phys. Chem. A* **2000**, *104*, 8475.
19. Badger R. M.: *J. Chem. Phys.* **1934**, *2*, 128.
20. Badger R. M.: *J. Chem. Phys.* **1935**, *3*, 710.
21. Neumann R. M.: *Astrophys. J.* **1970**, *161*, 779.
22. Andrews L., Liang B.: *J. Am. Chem. Soc.* **2001**, *123*, 1997.